



## Possible crater-based pingos, paleolakes and periglacial landscapes at the high latitudes of Utopia Planitia, Mars

R.J. Soare, Susan J. Conway, G.D. Pearce, J.M. Dohm, P.M. Grindrod

### ► To cite this version:

R.J. Soare, Susan J. Conway, G.D. Pearce, J.M. Dohm, P.M. Grindrod. Possible crater-based pingos, paleolakes and periglacial landscapes at the high latitudes of Utopia Planitia, Mars. *Icarus*, 2013, 225 (2), pp.971-981. <10.1016/j.icarus.2012.08.041>. <insu-02276063>

**HAL Id: insu-02276063**

**<https://insu.hal.science/insu-02276063v1>**

Submitted on 24 Jun 2022

**HAL** is a multi-disciplinary open access archive for the deposit and dissemination of scientific research documents, whether they are published or not. The documents may come from teaching and research institutions in France or abroad, or from public or private research centers.

L'archive ouverte pluridisciplinaire **HAL**, est destinée au dépôt et à la diffusion de documents scientifiques de niveau recherche, publiés ou non, émanant des établissements d'enseignement et de recherche français ou étrangers, des laboratoires publics ou privés.



HAL Authorization

# Open Research Online

---

The Open University's repository of research publications and other research outputs

## Possible crater-based pingos, paleolakes and periglacial landscapes at the high latitudes of Utopia Planitia, Mars

### Journal Item

#### How to cite:

Soare, R. J.; Conway, S. J.; Pearce, G. D.; Dohm, J. M. and Grindrod, P. M. (2013). Possible crater-based pingos, paleolakes and periglacial landscapes at the high latitudes of Utopia Planitia, Mars. *Icarus*, 225(2) pp. 971–981.

For guidance on citations see [FAQs](#).

© 2012 Elsevier Inc.



<https://creativecommons.org/licenses/by-nc-nd/4.0/>

Version: Accepted Manuscript

Link(s) to article on publisher's website:

<http://dx.doi.org/doi:10.1016/j.icarus.2012.08.041>

---

Copyright and Moral Rights for the articles on this site are retained by the individual authors and/or other copyright owners. For more information on Open Research Online's data [policy](#) on reuse of materials please consult the policies page.

---

[oro.open.ac.uk](http://oro.open.ac.uk)

## Accepted Manuscript

Possible crater-based pingos, paleolakes and periglacial landscapes at the high latitudes of Utopia Planitia, Mars

R.J. Soare, S.J. Conway, G.D. Pearce, J.M. Dohm, P.M. Grindrod

PII: S0019-1035(12)00360-0

DOI: <http://dx.doi.org/10.1016/j.icarus.2012.08.041>

Reference: YICAR 10367

To appear in: *Icarus*



Please cite this article as: Soare, R.J., Conway, S.J., Pearce, G.D., Dohm, J.M., Grindrod, P.M., Possible crater-based pingos, paleolakes and periglacial landscapes at the high latitudes of Utopia Planitia, Mars, *Icarus* (2012), doi: <http://dx.doi.org/10.1016/j.icarus.2012.08.041>

This is a PDF file of an unedited manuscript that has been accepted for publication. As a service to our customers we are providing this early version of the manuscript. The manuscript will undergo copyediting, typesetting, and review of the resulting proof before it is published in its final form. Please note that during the production process errors may be discovered which could affect the content, and all legal disclaimers that apply to the journal pertain.

**Possible crater-based pingos, paleolakes and periglacial landscapes at  
the high latitudes of Utopia Planitia, Mars**

R.J. Soare<sup>1</sup>, S.J. Conway<sup>2a,b</sup>, G.D. Pearce<sup>1</sup>, J.M. Dohm<sup>3</sup>, P.M. Grindrod<sup>4</sup>

<sup>1</sup>Department of Geography, Dawson College  
3040 Sherbrooke Street West, Montreal, Quebec, Canada, H3Z 1A4  
rsoare@dawsoncollege.qc.ca

<sup>2a</sup>Department of Physical Sciences, Open University  
Walton Hall, Milton Keynes  
UK, MK7 6AA  
(presently at)

<sup>2b</sup>LPGN, CNRS/Université Nantes 44322  
Nantes, France; 3 UMR 8148  
(work done at)

<sup>3</sup>Department of Hydrology & Water Resources  
University of Arizona, USA, 85721

<sup>4</sup>Department of Earth Sciences, University College, London  
Gower Street, London, UK. WC1E 6BT

**Pages:** 28

**Figs:** 13 (including a supplementary figure)

**Tables:** 2

**Abstract**

Closed-system pingos (CSPs) are perennial ice-cored mounds that evolve in relatively deep and continuous permafrost. They occur where thermokarst lakes either have lost or are losing their water by drainage, evaporation or sublimation and form by means of freeze-thaw cycling, permafrost aggradation and pore-water migration. The presence of CSPs on Mars, particularly on late-Amazonian Epoch terrain at near-polar latitudes, would indicate: 1. the antecedent occurrence of ponded water at the mound-formation sites; 2. freeze-thaw cycling of this water; and, 3. boundary-conditions of pressure and temperature at or above the triple point of water much more recently and further to the north than has been thought possible.

In 2005 we studied two crater-floor landscapes in northern Utopia Planitia and used MOC narrow-angle images to describe mounds within these landscapes that shared a suite of geological characteristics with CSPs on Earth. Here, we show the results of a circum-global search for similar crater-floor landscapes at latitudes  $> 55^{\circ}\text{N}$ . The search incorporates all relevant MOC and HiRISE images released since 2005. In addition to the two periglacially suggestive crater-floor landscapes observed by us earlier, we have identified three other crater floors with similar landscapes. Interestingly, each of the five mound-bearing craters occur within a tight latitudinal-band ( $64\text{--}69^{\circ}\text{N}$ ); this could be a marker of periglacial landscape-modification on a regional scale.

Just to the north of the crater-based pingo-like mounds Conway et al. (2012) have identified large (km-scale) crater-based perennial ice-domes. They propose that the ice domes develop when regional polar-winds transport and precipitate icy material onto the floor of their host craters. Under a slightly different obliquity-solution ice domes could have accumulated at the lower latitudes where the putative CSPs have been observed. Subsequently, were

temperatures to have migrated close to or at 0°C the ice domes could have thawed, forming endogenic paleolakes. This region also contains a significant concentration of crater-floor polygons. The polygons are thought to have formed by desiccation (El Maarry et al., 2010, 2012) or thermal contraction (Soare et al., 2005); on Earth each of these processes is associated with the end-stage of lake evolution.

On the basis of our enhanced image collection, a new map displaying the global distribution of mound-bearing craters and a two new digital-elevation models of a crater-floor with pingo-like mounds, we evaluate the CSP hypothesis anew. We also explore two alternative hypotheses: 1. the mounds are weathered central-uplift complexes; or, 2. they are impact-related hydrothermal structures. However, we propose that the CSP hypothesis is much more robust than these alternatives, encompassing geomorphological, cartographical, stratigraphical and climatological observations, and less subject to inconsistencies.

**Key words:** Mars climate, polar geology, surface

## **1. Introduction**

Closed-system (hydrostatic) pingos (CSPs) are perennial ice-cored hills or mounds. They evolve and persist only in permafrost, i.e. ground that is frozen for periods of no less than two years, that is continuous and relatively deep (Washburn, 1973; Harris et al., 1988; Mackay, 1998; French, 2007). CSPs are tens of metres in height and have basal diameters that reach hundreds of metres in some instances (**Fig. 1**). Their shape ranges from circular to sub-circular to elongate (**Fig. 1**). Other landforms such as small-sized polygons ( $\leq 40\text{m}$  in diameter) (**Fig. 2g**) formed by means of thermal-contraction cracking, and polygon-trough/junction pits, often are observed in close spatial-association with CSPs (Washburn, 1973; Mackay, 1998; French, 2007) (**Fig. 2b**).

On Earth, CSPs occur in regions such as the Tuktoyaktuk Coastlands (TC) of northern Canada where thermokarst lakes either have lost or are losing their water by drainage, evaporation or sublimation (e.g. Harris et al., 1988; Mackay, 1998) (**Figs. 2a-e; f-h**). They are the product of seasonal freeze-thaw cycling (as are the ice-wedges that underlie the small-sized polygons with which they may be associated spatially), permafrost aggradation and soil-moisture (pore-water) migration (Washburn, 1973; Mackay, 1998; French, 2007).

The identification of closed-system pingos on Mars, particularly on late-Amazonian Epoch terrain at or near-polar latitudes would point to: 1. the antecedent occurrence of ponded water at the mound-formation sites; 2. freeze-thaw cycling of this water; and, 3. boundary-conditions of pressure and temperature at or above the triple point of water much more recently and further to the north than many workers have thought possible.

In 2005 a small set of narrow-angle MOC (Mars Orbiter Camera, Mars Global Surveyor) images were used to describe two crater-floor landscapes in northern Utopia Planitia (UP) that showed mounds with morphological characteristics and landform associations similar to the CSPs of the TC (Soare et al., 2005a; 2005b). The images covered only a part of the crater floors. Using all relevant HiRISE (Mars Reconnaissance Orbiter, High Resolution Imaging Science Experiment) and MOC images (not available at the time of our earlier work and exhibiting complete crater-floor coverage) we have performed a circum-global search for similar crater-floor landscapes at latitudes  $> 55^{\circ}\text{N}$ . Three other crater floors that show similar landscapes have been identified. Interestingly, all of the mound-bearing craters are located within a tight latitudinal-band ( $64\text{--}69^{\circ}\text{N}$ ), centred in northern UP (**Fig. 3, Table 1**). This could be a marker of landscape-modification on a regional scale.

Just to the north of the pingo-like mounds Conway et al. (2012) have identified large (km-scale) crater-based perennial ice-domes in a near-polar latitudinal band ( $\sim 70^\circ\text{N}$ ). They propose that the ice domes are the product of regional polar-winds that transport and precipitate icy material onto the floor of their host craters. Under a slightly different obliquity-solution the same process could have occurred further to the south, in those craters where the putative closed-system pingos have been observed. Subsequently, were temperatures to have migrated close to or at  $0^\circ\text{C}$  the ice domes could have thawed, forming endogenic paleolakes. This region also contains a significant concentration of crater-floor polygons with diameters  $\leq 350\text{m}$ . The polygons are thought to have formed by desiccation (El Maarry et al., 2010, 2012) or thermal contraction (Soare et al., 2005); on Earth, each of these processes is associated with the end-stage of lake evolution.

Using an enhanced image collection, a new map displaying the global distribution of mound-bearing craters and two new digital-elevation models of a crater-floor with pingo-like mounds, we evaluate the CSP hypothesis anew. We also explore two alternative hypotheses: 1. the mounds are weathered central-uplift complexes; or, 2. they are impact-related hydrothermal structures.

## 2. *Methods*

As noted in the introduction, Soare et al. (2005a, b) employed narrow-angle MOC images ( $\sim 3\text{-}6\text{m/pixel}$ ) to identify, discuss and map two crater-floor landscapes with putative CSPs in northern UP. At the time, narrow-band and high-resolution image coverage of the study region -  $55\text{-}70^\circ\text{N}$  and  $60\text{-}120^\circ\text{E}$  - was incomplete. Thus, there were significant gaps in our map and intriguing as the CSP hypothesis appeared to be, its validation was beyond the compass of available data.



Now, all of the relevant MOC and HiRISE images of this region that were not available in 2005 are integrated with the more continuous impact-crater data collected by Conway et al. (2012) from MOLA (Mars Orbiter Laser Altimeter, Mars Global Surveyor) coverage. Moreover, we use all available HiRISE images (30-60cm/pixel) to extend the longitudinal reach of our study zone from a regional perspective to a circumpolar one (i.e., from 60° of coverage to 360°). Within this transect all imaged craters exhibiting diameters >7km were inspected for mounds.

The depth-diameter data for the craters in the region are derived as follows. Intact crater rims are digitised in MOLA data using the watershed methods detailed in Conway et al. (2012) and from this the centre-points calculated. The crater depths are taken as the lowest point on crater floor to the highest point on the rim according to gridded MOLA data and the diameters are estimated by calculating the average centre-to-rim distance (for more detail see Conway et al. 2012).

Within each of the mound-bearing craters, all of the mounds are mapped. Where topographic data of the craters were available, the crater-floor mounds are identified as discrete rises from the crater floor, noted by a distinct break in slope. In the absence of topographic data the shadows cast by the mounds are relied on for identification; thus, the estimate for these craters is conservative. Mound-distribution density is calculated by means of four steps. 1. identifying the location of the mound(s) furthest from the crater-floor centre; 2. measuring the radius between the two points; 3. using this radial distance and, derivatively, circumference to calculate floor-surface area (km<sup>2</sup>); and, 4. dividing the surface area by the number of mounds located therein. Mound heights for two of the studied craters are measured using elevation data derived from HiRISE stereo-pairs (ESP\_017525\_2475, ESP\_017090\_2475 and ESP\_018210\_2445, ESP\_018078\_2445) using the methods described by Kirk et al. (2008) at the

NASA RPIF3D facility at UCL. Using the method of Okubo (2010), we estimate the vertical precision of these two DEMs to be 0.23m and 0.18m respectively. Only mounds that are not clustered tightly with others are used for height measurements so as to obtain a reliable base-height. Heights are taken as the difference between highest and lowest elevation value within the polygon delimiting the mound. Our discussion integrates the spatial location of craters containing paleo-lakes as presented in Table 1 of El Maarry et al. (2010). The set of craters analyzed in this investigation is a subset of the population discussed in their recent study.

### **3. Mound morphology, traits and spatially associated crater-floor features in northern Utopia Planitia**

Pingo-like mounds are ubiquitous on Mars, albeit mainly at mid or equatorial latitudes (Dundas et al., 2010), and have been discussed by a multiplicity of workers: i.e. Acidalia Planitia (Lucchitta, 1981); the Athabasca Valles and the Cerberus Plains (Burr et al., 2005; Page and Murray, 2006; Page, 2007; Balme and Gallagher, 2009), Maja Valles (Theilig and Greeley, 1979); and mid Utopia Planitia (Dundas et al., 2008; Burr et al., 2009; de Pablo and Komatsu, 2009; Lefort et al., 2009; Dundas and McEwen, 2010). By contrast, the putative CSPs observed by us occur uniquely at near-polar latitudes in the northern hemisphere ( 64-69°N) (**Fig. 3**).

Through the past few years Bruno et al. (2006), Dundas et al. (2008, 2010) and Burr et al. (2009a, b) have urged caution in the reporting of pingo-like mounds and suggested that much work remains before pingo hypotheses are validated. In particular, Dundas et al. (2010) points to the apparent contradiction between a late-Amazonian Epoch that is thought to be highly arid and the water volume requirements of pingo hypotheses. We address some of their concerns below (cf. section 4.3.2).

In our study region (a circum-global transect comprising 55-70°N), the floors or basins of five impact-craters show spatially-associated complexes of small-sized unsorted polygons and mounds whose size, shape, key geological characteristics and distribution are consistent with thermokarst-lake or alas/CSP assemblages such as those located in the TC (**Fig. 3**). Table 1 presents the images used for each of these craters in the following analyses.

Host crater-diameters range from 7-19km (**Table 2**) and none of their ejecta deposits exhibit inward-oriented breaches or flow features. Sixty-seven other craters at or above the minimum crater diameter of 7km were imaged by the MOC and HiRISE cameras but did not show spatially-associated complexes of polygons and mounds. Host crater-depths are shallow compared with global crater depth-diameter estimates (Garvin et al., 2003)(**Fig. 4, Table 2**). However, this is consistent with the measurements of crater depths in the 10-25km diameter range above 52°N made by Kreslavsky and Head (2006). Intriguingly, each of the polygon and mound-bearing craters occur in northern UP within a tight latitudinal band (~64-69°N) and a narrow longitudinal reach (~26-98°E). This could be indicative of surface and/or atmospheric boundary conditions that are highly localised and possibly consistent with landscape modification by periglacial processes.

Mound diameters range from tens to hundreds of metres (**Figs. 5 and 6, Table 2**); mound heights extend from ~6-33m (**Table 2, Fig. 5**). In cross-section, the mounds are conical to domical in shape and have low flank-slopes of up to ~15° (**Fig. 5**). We do not observe summit fractures as seen in many pingos in TC but occasionally circular raised-rims with basal diameters similar to those of the crater-floor mounds are observed in proximity to these mounds (**Fig. 6**). These could be mound remnants or slump markers. Mound shape in plan view is circular to elongate (**Figs. 5 and 6**); mound distribution is clustered around or at the crater-floor centres.

Mound density in **Fig. 5** is  $\sim 0.9$  mounds/km<sup>2</sup> and 0.4 mounds/km<sup>2</sup> in **Fig. 6** (also, cf. supplementary **Figure 1**). Some mounds are nested directly on the crater floor; others, seem to lie atop ridge-like structures that show a ring-like appearance (**Fig. 6**).

All of the mound-bearing craters display floors dominated by unsorted polygonal-patterned ground  $\leq 350$ m in diameter (**Fig. 6**). Polygonisation is typical of the terrain within and around impact craters at this latitude (Gallagher et al., 2011). Some of crater-floor polygons cross-cut the mounds (**Fig. 5C**); others show an orthogonal orientation (**Fig. 6**). Recent estimates of crater-retention ages at this latitude, using the Heimdal Crater (68.3°N; 235.2°E) as a benchmark, suggest that the polygonised terrain is within the 0.5-2.0 Ma range (Gallagher et al., 2011).

#### 4. Discussion - Mound Origins

Here we consider three mound-formation hypotheses in the light of our new observations as well as the recent work of Conway et al. (2012) and El Maarry et al. (2010, 2012).

##### 4.1 Weathered uplift-complexes

On Mars, small ( $< 5$ km) impact craters are noted for having a relatively simple, bowl-shaped geometry (Werner et al., 2004; Wood et al., 1978). Large craters, particularly those above the  $\sim 8$ -10km range of diameter, exhibit complex morphologies that include terraced walls and regions of central uplift (Garvin et al., 2003; Wood and Andersson, 1978). Central uplift occurs in the modification and collapse phase of crater formation, following the formation of a transient cavity, as weak material collapses and returns to a state of gravitational equilibrium (Bond, 1981; Melosh, 1989). Regions of central uplift are typically domical, have one or several peaks, and exhibit maximum heights that are well below crater-rim crests and the level of surrounding plains (Bond, 1981).

There are two general observations suggesting that the observed mounds are weathered and/or partially-buried remnants of central-uplift material: 1. the mounds are clustered in the central region of the crater floors; and, 2. the craters in which they lie are above the threshold diameter for central-uplift formation. Under this scenario the central-uplift structures or complexes would have gradually undergone burial by sedimentation; once the crater-fill was sufficiently thick only the uplift summits would be visible, somewhat like nunataks in the Antarctic (**Fig. 7**). Weathering and erosion could have carved these structures into mounds similar in appearance to the ones observed on the crater-floors of UP. This scenario is consistent with the fact that craters serve as traps for dust and regolith over time and that our studied craters are observed to have relatively shallow depths (**Fig. 4**). Some authors have suggested that high-northern craters might be filled with dusty-ice (e.g. Kreslavsky and Head, 2006) and/or sediments deposited during the presence of a northern ocean (e.g. Boyce et al., 2005).

The plausibility of the central-uplift hypothesis is contingent upon crater-fill levels lying below the upper elevation-threshold of impact-related crater-floor structures. Even though accurate *in situ* measurements of fill depths are not available, estimates of fill depth can be calculated by using 1. MOLA profiles to identify crater diameters and rim elevations; and, 2. generally-accepted assumptions concerning the depth-to-diameter dimensions of complex craters. The latter comprise the following:

(a) Crater diameter is stable over time, changing by no more than 10-15% from its initial value as craters degrade (Craddock and Maxwell, 1990).

(b) Crater depth is diameter dependent and relatively accurate predictions of initial crater depth can be made from generalized formulae (Boyce et al., 2005; Garvin et al., 2003; Stewart and Valiant 2006).

(c) The height of central-uplift structures is diameter dependent and is well below the level of the surrounding plains (Garvin et al., 2003; Werner et al., 2004).

Using these assumptions we have identified five key characteristics of the five principal mound-bearing craters and summarise them here; more detail is available in Table 2: 1. rim-to-floor/top of fill depth (actual); 2. initial depth (estimated); 3. initial depth (estimated) to current floor (actual); 4. central-peak height (estimated); and, 5. height difference (estimated) between the current floor (actual) and the central-peak summit (estimated). Each of the mound-bearing craters show a minimum height difference of ~600m between the fill/crater floor level and the buried summit of the crater's central peak (**Table 2**). This difference of height is exemplified by comparing a MOLA profile that crosses the crater floor and central peak of a non mound-bearing complex crater in the northern plains (**Fig. 8a**) with a MOLA profile that crosses one of the five mound-bearing craters in the region (**Fig. 8b**).

As the crater-floor mounds and spatially-associated ridges occur well above the heights predicted for central peaks in each of the mound-bearing craters, this suggests that the mounds and ridges could not be partially-exposed central peaks or peak remnants. Interestingly, Stewart and Valiant (2006) suggest that Garvin's formulae underestimate the initial depth of complex impact-craters in some areas of the northern plains.

Are the initial depths of impact craters in the high northern plains shallower than elsewhere on Mars? Based on the following observations this seems unlikely: 1. the morphological traits associated with the high-northern craters, such as ejecta smoothing, are consistent with them having experienced high levels of infilling and modification (Garvin et al., 2003; Kreslavsky and Head, 2006); 2. there are some relatively pristine craters (distinguished by rough and easily visible ejecta-blankets) in this region that have depths exceeding the predicted

initial depth for craters with specific diameters derived of global averages (Garvin et al., 2003)(**Fig. 4**); and, 3. although variation in the lithology of impact targets has an influence on initial crater geometry (e.g., as summarized in Stewart and Valiant, 2006), significant infilling is still implied by the shallow depths observed in the mound-bearing craters compared to other craters in the surrounding area (**Fig. 4**).

Finally, if we consider that the craters in our study are outliers to the general population and therefore anomalously shallow then does the small-scale morphology of the mounds make sense as central complex remnants? Without a concrete example of a deeply buried central-uplift elsewhere on Mars we cannot compare directly the dimensions and density of mounds that we observe in UP. However, for craters 2 and 5 in particular it seems unlikely that a central-uplift complex could possess so many and such widely distributed (from the crater centre to within ~2km of the crater rim) peaks of almost the same height.

In summary, it is unlikely that these mounds are remnants of central uplift complexes, because the implied level of fill surpasses estimated uplift-elevations by over 600m (**Table 2**); moreover, in some cases the mound morphology is not consistent with the expected morphology of buried central-uplift complexes.

#### **4.2 Impact-related hydrothermal structures**

Impact-related hydrothermal activity (Newsom, 1980) could be the progenitor of the crater-floor mounds. For example, amongst the geological traits observed at the Hesperian-aged Toro impact crater on the northern edge of the Syrtis Major Volcanic Plains (17.0°E; 289.2°N) are mounds, polygonal fractures, veins and structural discontinuities that could be the result of volatile release and/or liquid flows (Fairen et al., 2010; Marzo et al., 2010). Distinctive mineralogy and abundances of hydrated phases in and around the central-uplift complex, perhaps

associated with impact-melt bearing crater-fill deposits, also are consistent with a hydrothermal origin of these structures (Marzo et al., 2010). The mounds and polygonal cracks observed here have similar dimensions to those that we observe in UP (**Fig. 9**); however, the close spatial-association of the mounds and polygons is not observed.

By a similar argument to that which is made for the central-uplift remnant hypothesis, the hydrothermal hypothesis can also be rejected. Although some of the crater fill in the mound-bearing craters could be associated with the impact formation of the craters themselves, the fill height of these craters exceeds the hypothesised level of impact-related melt material as well as central peak summits. For example, Toro crater is ~40km in diameter, has a rim to floor depth of ~2km and the central-peak summit rises 400m above the current crater floor (Marzo et al., 2010). By fitting a planar surface through the MOLA data exterior to this crater's ejecta; we were able to estimate the elevation difference between the plains and the central peak as ~960m. This means that the elevation of the central-uplift structure and, derivatively, the impact-related fill deposits, lie well below the elevation datum of the surrounding plains. In addition, although the mounds in Toro are located near the centre of the crater they are not atop the central uplift; this is where you would expect them to be located if they were exposed sub-aerially subsequent to the infilling of the host crater. By contrast, the putative CSPs in northern UP lie atop hundreds of metres of fill, almost at the elevation datum of the surrounding plains (Soare et al., 2011b).

### ***4.3 Perennial ice-cored mounds (pingos)***

#### ***4.3.1 Thermokarst lakes on Earth and the possible origin of closed-system pingos***

In periglacial landscapes such as the TC, closed-system pingos form where thermokarst lakes either have lost or are in the process of losing their water by drainage or evaporation (Mackay, 1998) (**Fig. 1**). Exposure of the previously unfrozen lake-floor to freezing temperatures



leads to permafrost aggradation downwardly through the lake-floor sediments and inwardly from the lake margin (Mackay, 1998). As the permafrost aggrades, pore water is placed under increasing hydrostatic pressure and migrates away from the freezing fronts. Impelled by this pressure, the pore water uplifts and deforms the newly frozen lake-floor; this happens at or near the centre of the lake-floor where the permafrost is particularly thin and where small residual ponds may occur (Mackay, 1998). When the pore water (injection ice) freezes beneath the uplifted lake floor an ice-core forms, providing the buttress of a perennial sediment-covered mound or pingo (Washburn, 1973, Mackay, 1998; French, 2007)

Polygonal-patterned ground formed by thermal-contraction cracking often surrounds and cross-cuts the pingos (**Fig. 2b**); ice wedges, the product of seasonal thaw, underlie polygon margins or troughs. In some instances, the polygons may show an orthogonal orientation (Soare et al., 2008, 2011a); this is a marker of the episodic loss of water in a thermokarst lake (Lachenbruch, 1962). When their ice-cores degrade and the mounds undergo ablation, slump material forms a raised-rim mound remnant (**Fig. 2c**) (Mackay, 1998; Washburn, 1973).

The Martian crater-floor mounds approximate terrestrial CSPs (of the TC type) in shape, size and spatial association with small-sized polygonal patterned-ground. In a survey of 1247 pingos (of which 98% are estimated to be hydrostatic) in Arctic Coastal Plain, northern Alaska, Jones et al. (2012) find that pingo heights range from 2 to 21m (mean 4.6m), diameter 32 to 295m (mean 94m) and maximum density of 0.18 per km<sup>2</sup>. A similar study of 3109 mostly hydrostatic pingos in northern Asia (Grosse and Jones, 2011) found that pingo heights range from 2-37m (mean 4.8m), and have a maximum density of 0.28 per km<sup>2</sup>. Hence, the UP mounds are slightly larger on average compared to pingo populations on Earth but they do have a similar height-to-diameter ratio. The density of the UP pingos is slightly higher than that

reported in the Jones et al. (2012) and Grosse and Jones (2011) studies; however if we consider a single basin in TC, we obtain a density of 3 per km<sup>2</sup>, hence the measurement of the density of pingos is susceptible to the scale considered. Pingos undergoing degradation on Earth often possess summit cracks, but we do not observe this in UP. The absence of summit cracks on the mounds in UP does not rule them out as being pingos, as many pingos on Earth never reach the threshold of size and stress for this to occur.

Of the three hypotheses presented and discussed above, the periglacial or closed-pingo system hypothesis also is the only one that is stratigraphically consistent with the depth calculations (initial and actual) of the mound-bearing complex craters in northern UP. That is to say, if the pingo-like mounds comprise post-fill structures or structures associated with a post-fill revision of the near-surface regolith, then their occurrence atop the fill would be expected.

#### ***4.3.2 Late Amazonian crater-lakes and climatic water-ice accumulation***

In their recent work Conway et al. (2012) have documented eighteen (km-scale) impact craters at latitudes  $\geq 70^\circ\text{N}$  that host large (mostly km-scale) perennial domes. Spectral data acquired by the MEX OMEGA (Mars Express, Observatoire pour la Minéralogie, l'Eau, les Glaces et l'Activité) show high water-ice concentrations (up to 0.7 band depth) at the surface of some of these craters (Conway et al., 2012). None of the host craters are smaller than 9.5 km in diameter; ten craters exhibit diameters from 9.5-20km. The maximum thickness of their water-ice domes ranges from 94-1640m and the ice mound-summit-to-rim distance varies from 13-626m. Interestingly, each of the impact craters that show pingo-like mounds on their floors have diameters between 7.3-18.8 km (cf. Table 2).

Conway et al. (2012) hypothesise that these massive ice-domes form from water-ice vapour transported from the north-polar region and cold-trapped in their host craters (**Fig. 10**).

Cold-trapping could be triggered by the higher atmospheric pressure and lower temperature of crater interiors; in turn, this would increase the accumulation rates of water-ice during the winter. Were accumulation significant enough then this water-ice could be preserved through the spring and summer when the seasonal polar cap retreats, creating a perennial ice-dome. Once formed, the ice domes comprise a positive feedback-loop whereby their high albedo and high thermal-inertia but low temperatures are a permanent cold trap for condensation.

Similar domes could have evolved in the craters where the putative CSPs occur, under orbital parameters where the stability zone of ice-dome formation extends slightly further to the south than is the case currently (  $64^{\circ}\text{N}$ , according to the southern-most crater where the CSPs are located). This is likely to be a period with higher obliquity and/or eccentricity that lengthens the northern-winter. When Mars returns to antecedent orbital-parameters the stability zone of ice-dome formation in the northern hemisphere would migrate polewardly; depending upon regional boundary conditions the more southerly domes either would sublimate or thaw, pool and form endogenic paleo-lakes.

Indirect evidence of paleo-lakes having formed at the latitudes of the current ice-domes and the putative CSPs has been reported by El Maarry et al. (2008, 2010). They have studied the fracture mechanics of crater-floor polygons at near-polar latitudes in the northern hemisphere of Mars. The polygons range in diameter from  $\sim 15\text{-}350\text{m}$  and are located principally between  $65\text{-}75^{\circ}\text{N}$  (El Maarry et al., 2010)(**Fig. 3**). El Maarry et al. (2010) hypothesise that under present boundary conditions the crater-floor polygons with diameters  $\geq 75\text{m}$  can be formed only by desiccation, not by sublimation-related processes; if so, then this points to the antecedent occurrence of paleolakes in the host crater-basins (El Maarry et al., 2010). With regard to the crater-floor polygons  $\leq 75\text{ m}$ , their formation could be the result of desiccation (El Maarry et al.,

2010) or thermal contraction (El Maarry et al., 2010; also, Soare et al., 2005). Polygon formation by means of thermal-contraction cracking, particularly when the polygons exhibit an orthogonal orientation as some of them do in the putative CSP craters, also points to periglacial processes at work in a lacustrine environment (Lachenbruch, 1962).

Two other landscape characteristics are consistent with the antecedent occurrence of paleolakes in the CSP impact craters: ridge-like structures on the crater floors and the relative location of the CSPs themselves. With regard to the former, these might be sedimentary markers or paleo-shorelines of a lake in recession or of residual ponds forming prior to the complete loss of lake water on the crater floor. On the other hand these ridges could be indicative of a structural control on the migration of subsurface volatiles, as there is often a genetic/spatial linkage among tectonic (e.g., faults and joints), and emplaced (e.g., dikes and elongated plugs, hydrothermal mounds, migrating pingos) landforms (Dohm, 1995, Dohm et al., 2001; Tanaka et al., 1998; Wu et al., 2005).

With regard to the latter, and as noted above, the formation of CSPs on Earth tends to occur at or near the centre of a host thermokarst lake, this being the site of thin permafrost where remnant water pools last (Mackay, 1998). The putative Martian CSPs show clustering at or near the centre of their host craters that is consistent with terrestrial thermokarst-lake/CSPs assemblages (Fig. 1g).

A possible constraint on the CSP hypothesis concerns the availability of liquid water volumetrically sufficient to generate CSPs on crater floors at high northern latitudes (Dundas et al., 2010). However, the current thicknesses and summit-to-rim distances of ice domes in craters comparable in diameter to those hosting pingo-like mounds suggest that the water requirements of the latter can be met were pre-cursor ice-domes to have formed in the mound-bearing craters.

As noted above, ice dome thicknesses in craters with diameters of 9.5-20km ranges from tens to hundreds of metres and summit-to-rim distances comprise hundreds to thousands of metres in reach (Conway et al., 2012).

Using a DEM we have calculated the heights of two putative CSPs (15m, cf. Table 2). Even if one assumes a volumetric loss of 9% when water ice changes phase to liquid water as an ice dome thaws and melt-water pools on a crater floor, ice-dome thickness largely exceeds the height of the pingo-like mounds by an order of magnitude. In some instances, summit-to-rim distances also exceed mound diameters by an order of magnitude.

### **Conclusion**

Compared to the alternative hypotheses, the periglacial hypothesis is much more robust and coherent in explaining crater-floor mound formation in northern UP. It integrates geomorphological, stratigraphical and climatological observations, assumptions and estimates whereas the alternatives do not. Moreover, only the periglacial hypothesis is consistent with fill-depth estimates of the mound-bearing impact craters.

In terms of shape, size key geological characteristics and distribution, the crater-floor mounds of northern UP are consistent with the shape, size, key geological characteristics and distribution of CSPs in terrestrial periglacial-environments such as the Tuktoyaktuk Coastlands. Moreover, regardless of whether the small-sized polygons located in craters with pingo-like mounds are the result of desiccation or thermal contraction, both processes are associated with lake evolution on Earth and are consistent with the CSP hypothesis.

We suggest that the landscape assemblage comprised of crater-floor pingo-like mounds and small-sized polygons is a paleo-marker of freeze-thaw cycling and of a surface /near-surface system, albeit a highly localised one, rich in water. Consequently, the atmospheric boundary

conditions of temperature, atmospheric pressure and humidity required to initiate and maintain the freeze-thaw cycling of water would have been much higher than many workers have thought possible in the region during the late Amazonian Epoch.

### Acknowledgements

S.J.C's work was supported by a post-doctoral research grant from the Pays de Loire, France. P.M.G is funded by the UK Space Agency (Aurora Fellowship grants ST/F011830/1; ST/J002127/1; ST/J005215/1). The authors of this article would like to express their gratitude to Jeff Kargel and an anonymous reviewer for thoughtful comments that enabled us to improve our work substantially.

### References

- Balme, M.R., Gallagher, C., 2009. An equatorial periglacial landscape on Mars. *Earth and Planetary Science Letters* 285 (1-2) 1-15, doi:10.1016/j.epsl.2009.05.031.
- Bond, J. W., 1981. The development of central peaks in lunar craters, *The Moon, and the Planets* 25, 465-476.
- Boyce, J.M., Mougini-Mark, P., Garbeil, H. 2005. Ancient oceans in the northern lowlands of Mars: Evidence from impact crater depth/diameter relationships. *Journal of Geophysical Research*, 110 (E3) doi:10.1029/2004JE002328.
- Bruno, B.C., Fagents, S.A., Hamilton, C.W., Burr, D.M., Baloga, S.M., 2006. Identification of volcanic rootless cones, ice mounds, and impact crater on Earth and Mars: Using spatial distribution as a remote sensing tool. *Journal of Geophysical Research* 111, E06017, doi:10.1029/2005JE002510.
- Burr, D.M., Soare, R.J., Wan Bun Tseung, Emery, J.P., 2005. Young (late Amazonian) near-

surface ground-ice features near the equator. *Icarus* 178 (1) 56-73, doi:10.1016/2005.04.

012.

Burr, D.M., Bruno, B.C., Lanagan, P.D., Glaze, L.S., Jaeger, W.L., Soare, R.J., Wan Bun  
Tseung, J.M., Skinner, J.A., Baloga, S.M., 2009a. Mesoscale raised rim depressions  
(MRRDs) on earth: A review of the characteristics, processes, and spatial distribution of  
analogues for Mars. *Planetary and Space Science* 57, 5-6, 579-596,  
doi.org/10.1016/j.pss.2008.11.011.

Burr, D.M., Tanaka, K.L., Yoshikawa, K., 2009b. Pingos on Earth and Mars. *Planetary and  
Space Science* 57, 5-6, 541-555. doi.org/10.1016/j.pss.2008.11.003.

Conway, S.J., Hovius, N., Barnie, T., Besserer, J., Le Mouélic, S., Orosei, R., Read, N.A., 2012.  
Climate-driven deposition of water ice and the formation of mounds in craters in Mars'  
North Polar region. *Icarus* 220, 1, 174-193, dx.doi.org/10.1016/j.icarus.2012.04.021

Craddock, R.A., Maxwell, T.A., 1990. Resurfacing of the Martian highlands in the Amenthes  
and Tyrrhena Region. *Journal of Geophysical Research* 95 (B9) 14,265-14,278.

de Pablo, M.A., Komatsu, G., 2009. Possible pingo fields in the Utopia basin, Mars: Geological  
and climatic implications. *Icarus* 199 (1) 49-74, doi:10.1016/j.icarus.2008.09.007.

Dohm, J.M., 1995. Origin of Stoneman lake, and volcano-tectonic relations of Mormon  
and San Francisco volcanic fields, Arizona, M.S. thesis, Northern Arizona  
University, Flagstaff, Arizona, 101 p.

Dohm, J.M., Tanaka, K.L., Hare, T.M., 2001. Geologic map of the Thaumasia region of Mars.  
*USGS Misc. Inv. Ser.* Map I-2650, scale 1:5,000,000.

Dundas, C.M., Mellon, M.T., McEwen, A.S., Lefort, A., Keszthelyi, L.P., Thomas, N., 2008.

- HiRISE observations of fractured mounds: Possible Martian pingos. *Geophysical Research Letters* 35, L04201, doi:10.1029/2007GL031798.
- Dundas, C.M., McEwen, A.S., 2010. An assessment of evidence for pingos on Mars using HiRISE. *Icarus* 205, 244-258, doi:10.1016/j.icarus.2009.02.020.
- El Maarry, M.R., Markiewicz, W.J., Mellon, M.T., Goetz, W., Dohm, J.M., Pack, A., 2010. Crater Floor Polygons: Desiccation Patterns of Ancient Lakes on Mars? *Journal of Geophysical Research* 115 (E10006) doi:10.1029/2010JE003609.
- Fairén, A.G. et al., 2010. *Proceedings of the National Academy of Sciences* 107, 12,095-12,100, doi:10.1073/pnas.1002889107.
- French, H.M., 2007. *The periglacial environment*, 3<sup>rd</sup> edition. Wiley, West Sussex, England, 458 p.
- Gallagher, C., Balme, M.R., Conway, S.J., Grindrod, P.M., 2011. Sorted clasted stripes, lobes and associated gullies in high latitude craters on Mars: landforms indicative of very recent polycyclic ground-ice thaw and liquid flows. *Icarus* 211, 458-471. doi:10.1016/j.icarus.2010.09.010.
- Garvin, J.B., Sakimoto, S.E.H., Frawley, J.J., 2003. Craters on mars: global geometric properties from MOLA gridded topography. *6th Mars Conf.* Abstract # 3277.
- Grosse, G., Jones, B.M., 2011. Spatial distribution of pingos in northern Asia. *The Cryosphere* 5, 13-33, doi:10.5194/tc-5-13.
- Hamilton, T.D., Obi, C.M., 1982. Pingos in the Brooks Range, northern Alaska, USA. *Arctic and Alpine Research* 14 (1) 13-20.
- Harris, S.A. et al., 1988. Glossary of permafrost and related permafrost terms. Permafrost



- Subcommittee, Associated Committee on Geotechnical Research, National Research Council of Canada, Ottawa, Technical Memorandum 142, 156 p.
- Hauber, E., Reiss, Ulrich, M., Preusker, F., Trauthan, F., Zanetti, M., Hiesinger, H., Jaumann, R., Johansson, L., Johnsson, A., Van Gasselt, S., Olvmo, M., 2011. Landscape evolution in Martian mid-latitude regions: insights from analogous periglacial landforms in Svalbard. *Geological Society, London, Special Publications*, 356, 111-131, doi:10.1144/SP356.7.
- Jones, B M., Grosse, G., Hinkel, K.M., Arp, C.D., Walker, S., Beck, R.A., Galloway, J.P., 2012. Assessment of pingo distribution and morphometry using an IfSAR derived digital surface model, western Arctic Coastal Plain, Northern Alaska. *Geomorphology* 138 (1) 1-14. doi:10.1016/j.geomorph.2011.08.007.
- Kirk, R.L., Howington-Kraus, E., Rosiek, M.R., Anderson, J.A. , Archinal, B.A., Becker, K.J., Cook, D.A. et al., 2008. Ultrahigh resolution topographic mapping of Mars with MRO HiRISE stereo images: Meter-scale slopes of candidate Phoenix landing sites. *Journal of Geophysical Research (Planets)* 113, doi:10.1029/2007JE003000.
- Kreslavsky, M.A., Head, J.W., 2006. Modification of impact craters in the northern plains of Mars. Implications for Amazonian climate history. *Meteoritics and Planetary Science* 41 (10) 1633-1646.
- Lachenbruch, A.H., 1962. *GSA Special Paper 70*. New York: Geological Society of America, 69 p.
- Lefort, A., Russell, P.W., McEwen, A.S., Dundas, C.M., Kirk, R.L., 2009. Observations of periglacial landforms in Utopia Planitia with the High Resolution Imaging Science Experiment (HiRISE). *Journal of Geophysical Research* 114 (E04005) doi:10.1029/2008JE003264.

- 511 Lucchitta, B., 1981. Mars and Earth: comparison of cold-climate features. *Icarus* 45, 264-303.
- 512 Mackay, J.R., 1998. Pingo growth and collapse, Tuktoyaktuk peninsula area., western Arctic  
513 coast, Canada: a long-term study. *Géographie physique et Quaternaire* 52 (3) 1-53.
- 514 Marzo, G.A. et al., 2010. Evidence for Hesperian impact-induced hydrothermalism on Mars.  
515 *Icarus* 208 (2) 667-683, doi:j.icarus.2010.03.013.
- 516 Melosh, H.J., 1989. Impact cratering: a geologic process: New York, Oxford University Press,  
517 245 p.
- 518 Newsom, H.E., 1980. Hydrothermal alteration of impact melt-sheets with implications for  
519 Mars. *Icarus* 44, (1) 207-216.
- 520 Okubo, C.H., 2010. Structural geology of Amazonian-aged layered sedimentary  
521 deposits in southwest Candor Chasma, Mars. *Icarus* 207, 210-225, doi:10.1016/j.icarus.  
522 2009.11.012.
- 523 Page, D.P., 2007. Recent low-latitude freeze-thaw on Mars. *Icarus* 189 (1) 83-117, doi:10.1016/  
524 j.icarus.2007.01.005.
- 525 Page, D.P., Murray, J.B., 2006. Stratigraphical and morphological evidence for pingos in the  
526 Cerberus plains. *Icarus* 183 (1) 46-54, doi:10.1016/j.icarus.006.01.017.
- 527 Soare, R.J., Burr, D.M., Wan-Bun Tsueng, J.M., 2005a. Possible pingos and a periglacial  
528 landscape in Utopia Planitia, Mars. *Icarus* 174 (2) 373-382, doi:10.1016/j.icarus.2004.  
529 11.013.
- 530 Soare, R.J., Burr, D.M., Wan-Bun Tseung, J.M., Peloquin, C., 2005b. Possible pingos and  
531 periglacial landscapes in northwest Utopia Planitia. *LPS XXXVI*, Abstract # 1102.
- 532 Soare, R.J., Osinski, G.R., Roehm, C.L., 2008. Thermokarst lakes and ponds on Mars in the

- very recent (late Amazonian) past. *Earth and Planetary Science Letters* 272 (1-2) 382-393, doi:10.1016/j.epsl.2008.05.010.
- Soare, R.J., Séjourné, A., Pearce, G., Costard, F., Osinski, G.R., 2011a. The Tuktoyaktuk Coastlands of northern Canada: a possible “wet” periglacial analogue of Utopia Planitia, Mars. *Geological Society of America Special Paper* 483, doi:10.1130/2011.2483(13).
- Soare, R.J., Costard, F., Pearce, G., 2011b. Possible pingos and crater-floor periglacial landscapes in northwest Utopia Planitia: a re-assessed hypothesis based on Hi-RISE imagery. *LPS XXXII*, Abstract # 1364.
- Stewart, S.T., Valiant, G.J., 2006. Martian subsurface properties and crater formation processes inferred from fresh impact crater geometries. *Meteoritics and Planetary Science* 41 (10) 1509-1537, doi:10.1111/j.1945-5400.2006.tb00433.x
- Tanaka, K.L., Dohm, J.M., Lias, J.H., Hare, T.M., 1998. Erosional valleys in the Thaumasia region of Mars: hydrothermal and seismic origins. *Journal of Geophysical Research* 103, 31,407-31,419 doi:10.1029/98JEO1599.
- Theilig, E., Greeley, R., 1979. Plains and channels in the Lunae Planum-Chryse Planitia Region of Mars. *Journal of Geophysical Research* 84 (B14) 7994-8010.
- Washburn, A.L., 1973. *Periglacial processes and environments*. St. Martin's Press, New York, N.Y.
- Werner, S.C., Ivanov, B.A., Neukum, G., 2004. Impact cratering on Mars: Search for target influence on morphology. *LPS XXXV*, Abstract #1953.
- Wood, C.A., Head, J.W., Cintala, M.J., 1978. Interior morphology of fresh Martian craters-The effects of target characteristics. *LPS IX*, pp. 3691-3709.
- Wu, Z. et al., 2005. Migrating pingos in the permafrost region of the Tibetan Plateau, China and

their hazard along the Golmud-Lhasa railway. *Engineering Geology* 79 (3-4) doi:10.1016/j.enggeo.2005.02.003.

## Figures

1. The Pingo Canadian Landmark is a national park 6km southwest of Tuktoyaktuk adjacent to the Beaufort Sea in the Tuktoyaktuk Coastlands of northern Canada. Image (A27917-35-1993) courtesy of the Canadian Air Photo Library. Amongst the numerous pingos located here are Ibyuk (circular and ~49m in height) at the right; Split (sub-circular and ~ 35m in height) at the centre; and, an un-named elongated pingo at the top of the image on the left.
2. **a-e)** An idealised schema of closed-system pingo evolution in the Tuktoyaktuk Coastlands (TC) of northern Canada (Mackay, 1998). This is discussed in detail in Section 4.3.1. **f)** A small thermokarst lake surrounded by thermal-contraction polygons (TC, early July 2007). Image credit: R. Soare. **g)** A three-pingo complex in the midst of a thermokarst lake losing its water by evaporation and/or drainage. Note the un-vegetated and pale margins of the lake and pingos, indicative of water loss that is relatively recent (TC, early July 2007). Image credit: R. Soare. **h)** The end-stage of pingo evolution is a raised-rim landform or scar comprised of slump material, as exemplified by this oblique view of a collapsed pingo in the Brooks Mountains of Alaska (Hamilton and Obi, 1982).
3. Map showing the spatial distribution of mound-bearing impact craters in northern Utopia Planitia: the map incorporates a MOLA hillshade-background image (courtesy of [www.jpl.nasa.gov](http://www.jpl.nasa.gov)) and the following CTX images comprise the crater mosaic below the map: B02\_010392\_2491, P16\_007372\_2474, B22\_018078\_2445, P19\_008492\_2446, B19\_017089\_2341 and B19\_017154\_2472 (courtesy of MSSS/Caltech/JPL).

4. Depth-diameter plot of the craters in the region local to those containing mounds, i.e. 62-70°N and 26-98°E, as mapped by Conway et al. (2012). The craters with mounds and the craters mapped as containing evidence of crater lakes by El Maarry, et al. (2010) are highlighted. The depth-diameter relationship found by Garvin et al. (2003) is included as a reference.
5. Mounds on the floor of crater # 2, HiRISE image ESP\_017090\_2475 (courtesy of NASA/JPL/U of A) overlain on CTX image P16\_007372\_2474 (courtesy of MSSS/Caltech/JPL). 10m contours are derived from a 1m/pixel DEM produced from HiRISE images ESP\_017525\_2475, ESP\_017090\_2475. Online version has a color-drape which was derived from the HiRISE DEM. Stars indicate the locations of the mapped mounds used to produce the statistics in Table 2. Cross-sections whose locations are indicated on the image insets A-C are also derived from the same elevation data.
6. Mounds in crater # 3, HiRISE image PSP\_007780\_2450; 64.5°N, 63.7°E; 25 cm/pixel (courtesy of NASA/JPL/U of A). Note the diversity of mound morphology, highlighted in the white boxes: i) circular, ii) elongate and iii) remnant, possibly a mound scar. Clustering at or near the crater-floor centre is a keynote of mound distribution, as is a ring-like appearance.
7. Central peak of well-preserved crater northwest of Tartarus Montes: HiRISE PSP\_009240\_2055; 25.0°N, 167.6°E; 25 cm/pixel (courtesy of NASA/JPL/U of A).
8. **a)** Plan and profile view of a ~13.5km diameter mound-bearing crater at 67.2°N, 47.8°E. The solid black line is derived from MOLA profile 20037 and presents the level of the crater floor to be very near that of the surrounding plains. The serrated black line shows an estimate for the initial depth of the crater based on a power law derived from Garvin et al. (2003). CTX image P16\_007372\_2474 was used for the top of the figure (courtesy of CalTech/JPL). **b)**

Plan and profile view of a ~18.7km diameter crater with a central peak at 38.6°N, 137.2°E. MOLA profile 12352 crosses the crater's central peak, indicating that it is well below the level of the surrounding plains. Crater image is cropped from THEMIS visible wavelength image V09919018 (courtesy of NASA/JPL/ASU).

- 9.** Hydrothermal features on the floor of Toro crater (17.0°E; 289.2°N) in HiRISE image PSP\_005842\_1970 (courtesy of NASA/JPL/U of A). A) Small-scale mounds on the floor of Toro crater, marked by white arrows. B) Polygonal pattern on the floor of Toro crater.
- 10.** Oblique view of the ice dome in Korolev crater (~80km diameter). View is from the rim at 72.9°N, 162.6°E looking to the east. The elevation data used for this view are MOLA gridded data and the height of the dome from the trough is ~1 km. CTX images used: P21\_009042\_2528 and P20\_008831\_2529 (courtesy of MSSS/Caltech/JPL).

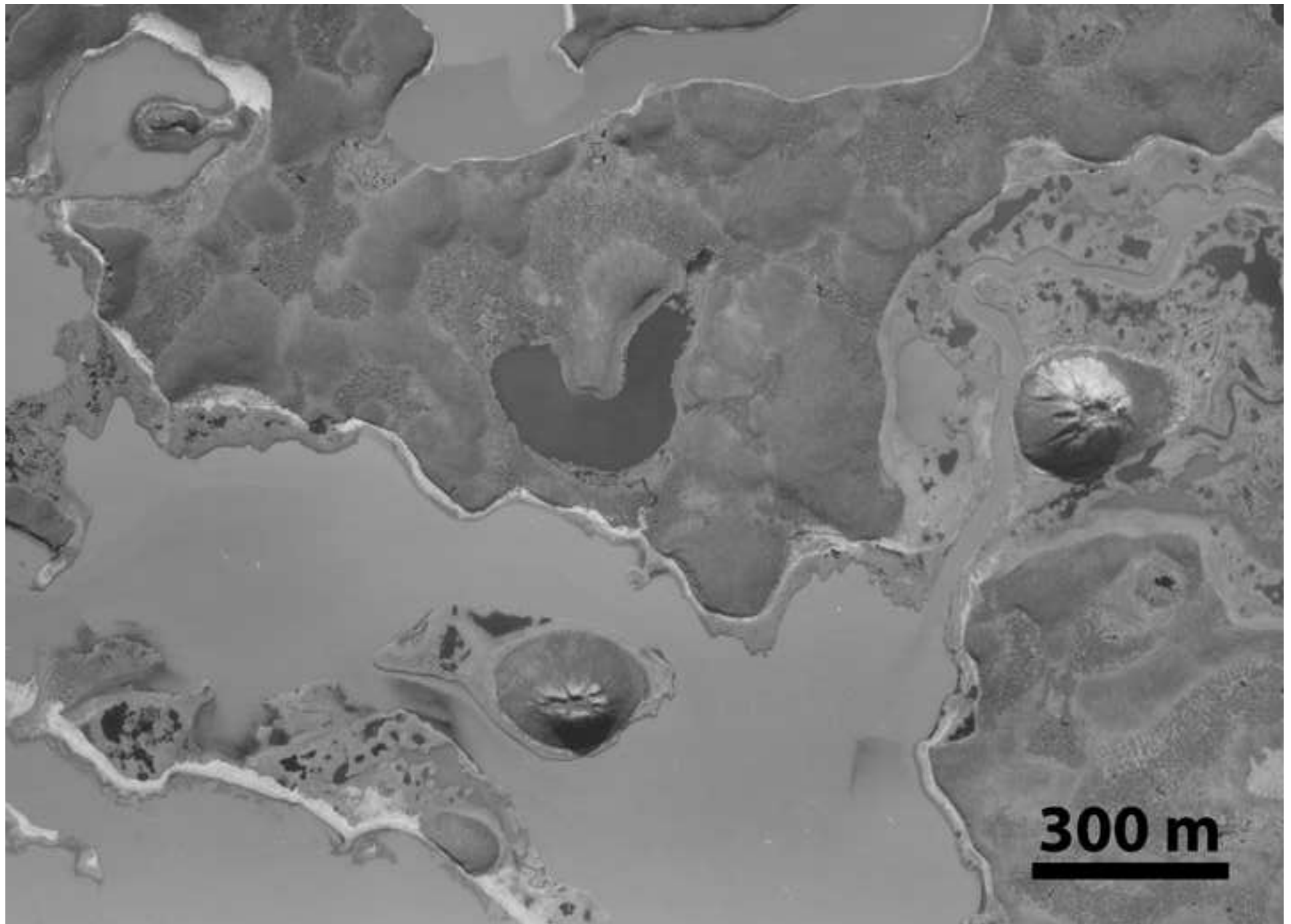
## Tables

**Table 1.** Crater floors studied in this article, their locations and the images used. Crater IDs marked with \* indicate those craters included in the Soare et al. (2005) study.

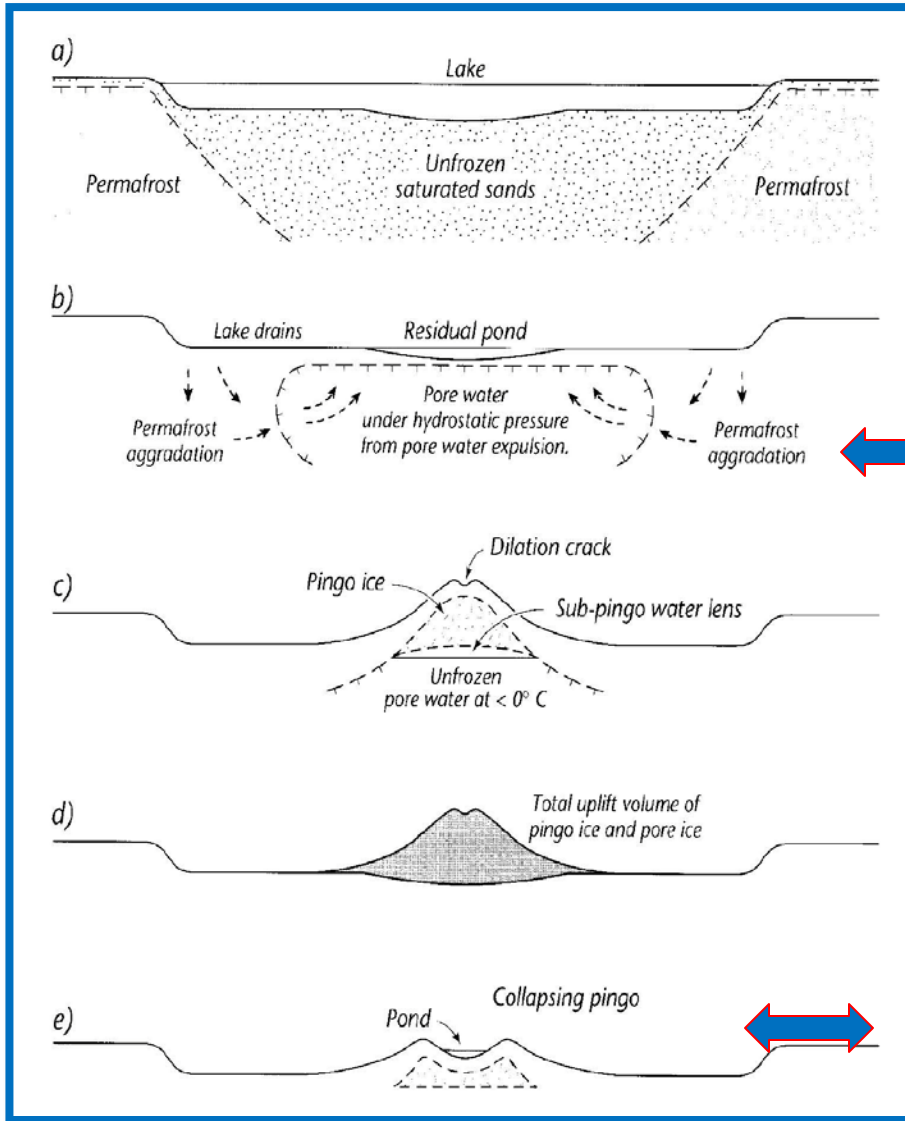
Crater ID	Latitude (°N)	Longitude (°E)	HiRISE images	MOC images	CTX images
1	68.945	26.760	PSP_008757_2490, ESP_017691_2910		B02_010392_2491
2	67.193	47.845	PSP_007372_2475, ESP_017525_2475, ESP_017090_2475		P16_007372_2474
3*	64.476	67.285	PSP_008492_2450, PSP_007780_2450	E0300299	P19_008492_2446
4*	64.324	70.378	ESP_015942_2445, ESP_018210_2445, ESP_018078_2445	E0500113	B22_018078_2445
5	67.131	97.547	ESP_017009_2475, ESP_017154_2475, ESP_017576_2475		B19_017154_2472

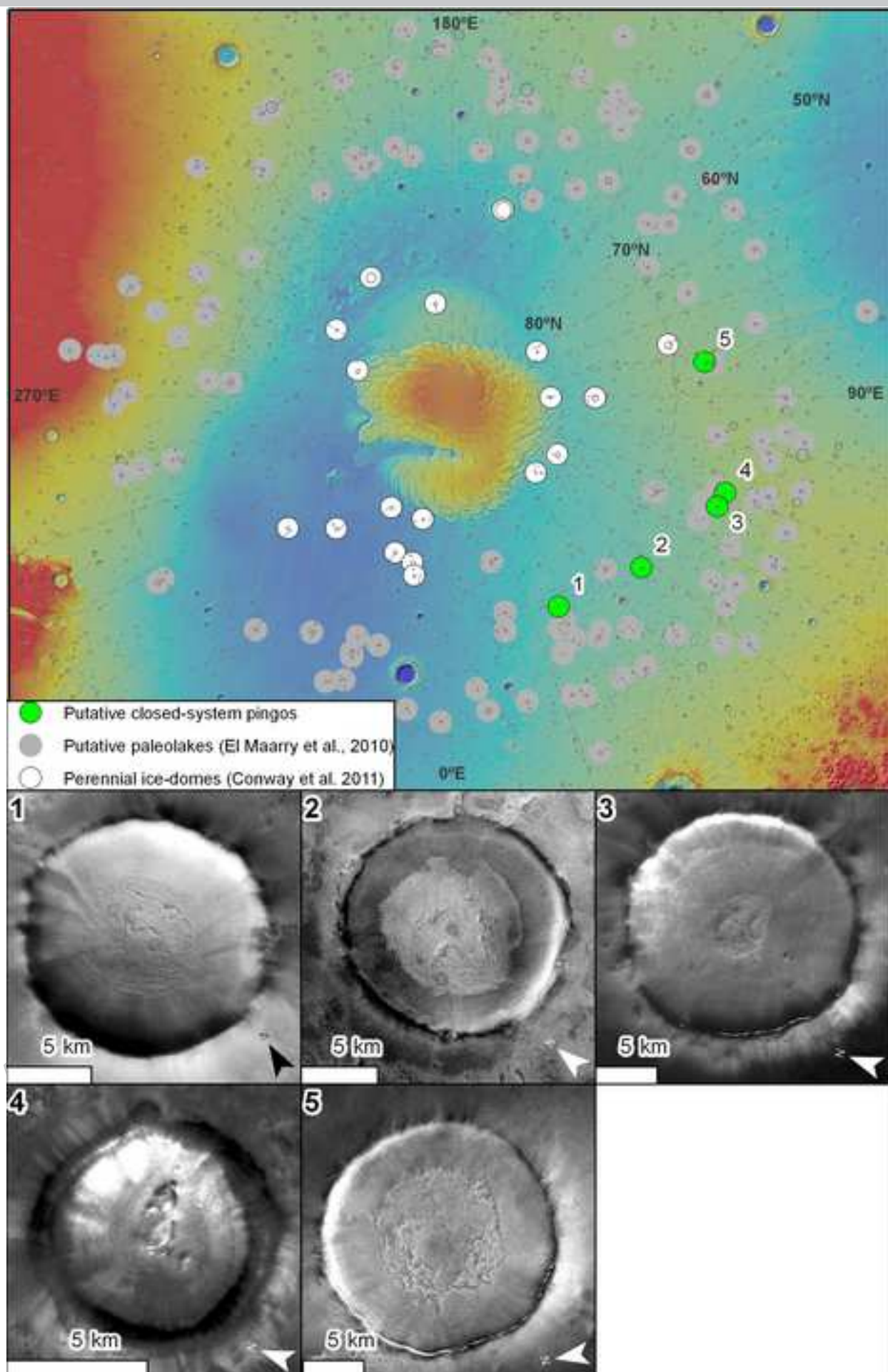
**Table 2.** Characteristics of craters containing mounds and the mounds themselves. Crater-elevation data are taken from MOLA and mound-elevation data are taken from HiRISE stereo-elevation models (cf. supplementary Figure 1).

Crater ID	Depth (m)	Diameter (km)	Predicted depth from Garvin et al. (2003) (m)	Estimated fill thickness (m)	Central uplift height from Garvin et al. (2003) (m)	Estimated elevation difference - central uplift to surface (m)	# of mounds (# used for height measurements)	Aerial extent of mound-basin (km <sup>2</sup> )	Mound density (#/km <sup>2</sup> )	Mean height in metres (range)	Mean diameter in metres (range)
1	553	14.0	1312	759	154	605	13	30	0.43		
2	437	14.1	1316	879	154	725	44 (16)	51	0.86	15 (6-33)	278 (186-458)
3	518	18.2	1492	974	176	798	36	128	0.28		
4	218	7.3	954	736	110	625	8 (8)	12	0.67	15 (8-22)	194 (86-366)
5	446	18.8	1516	1070	179	891	68	105	0.65		

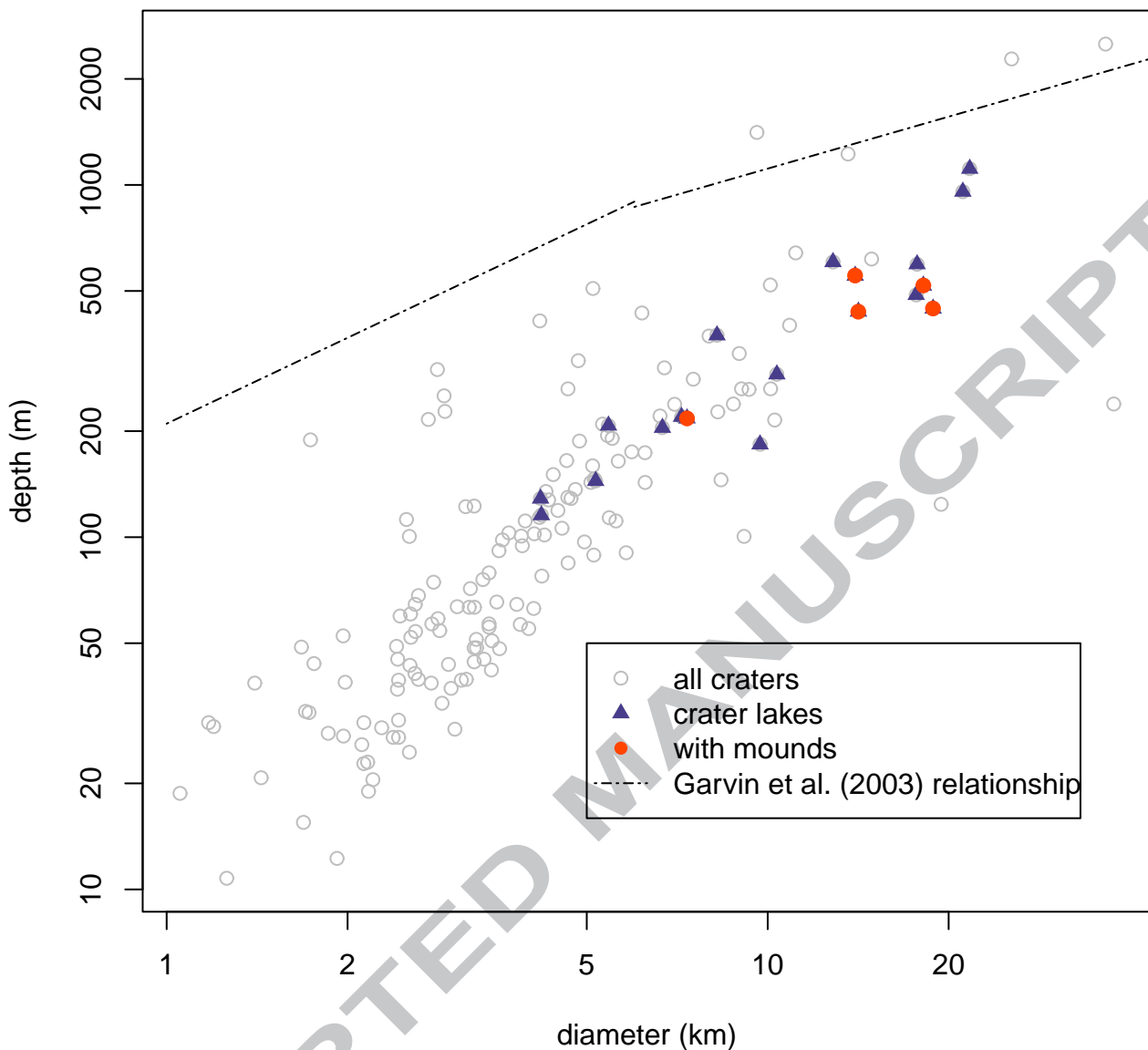




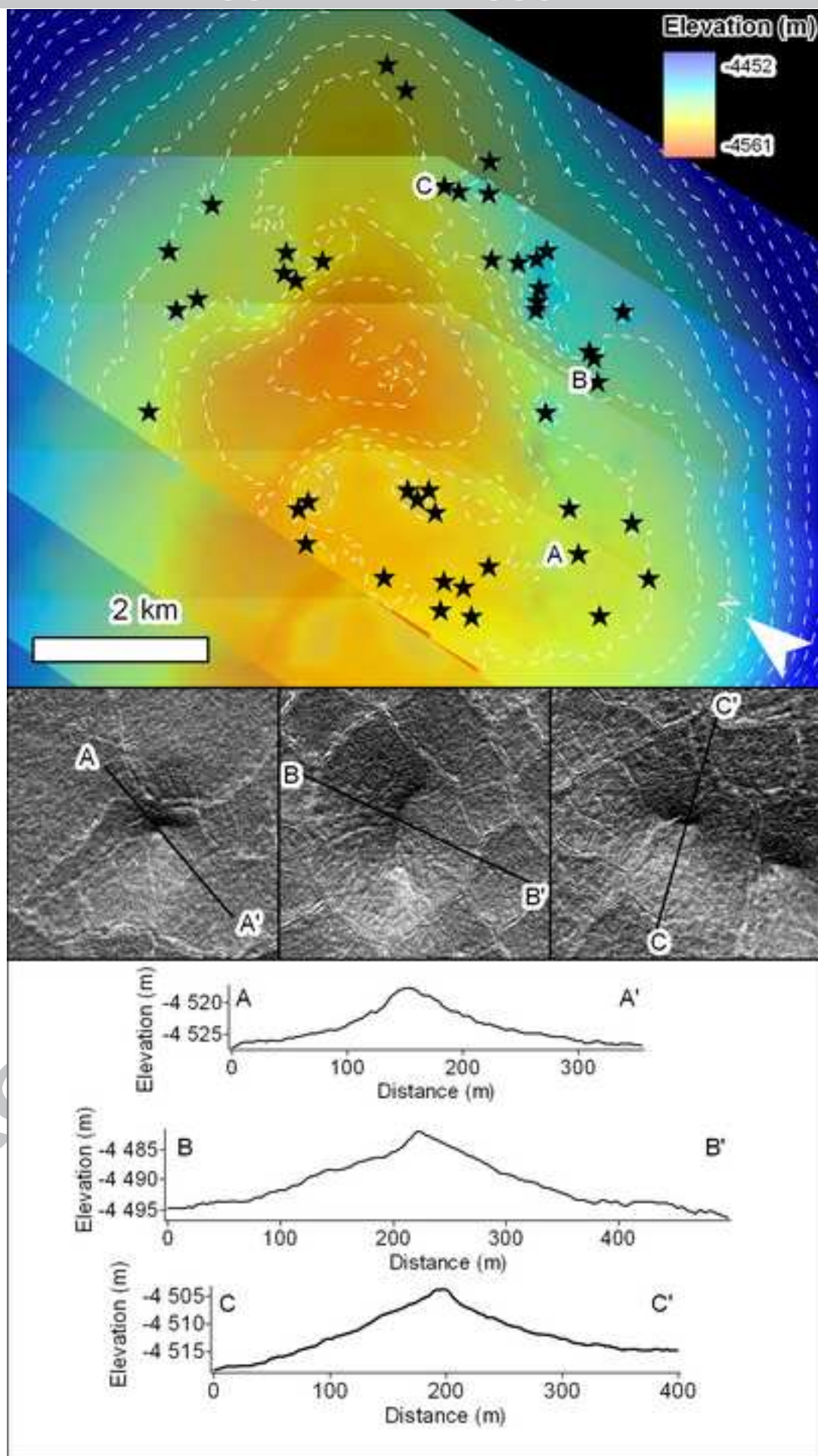


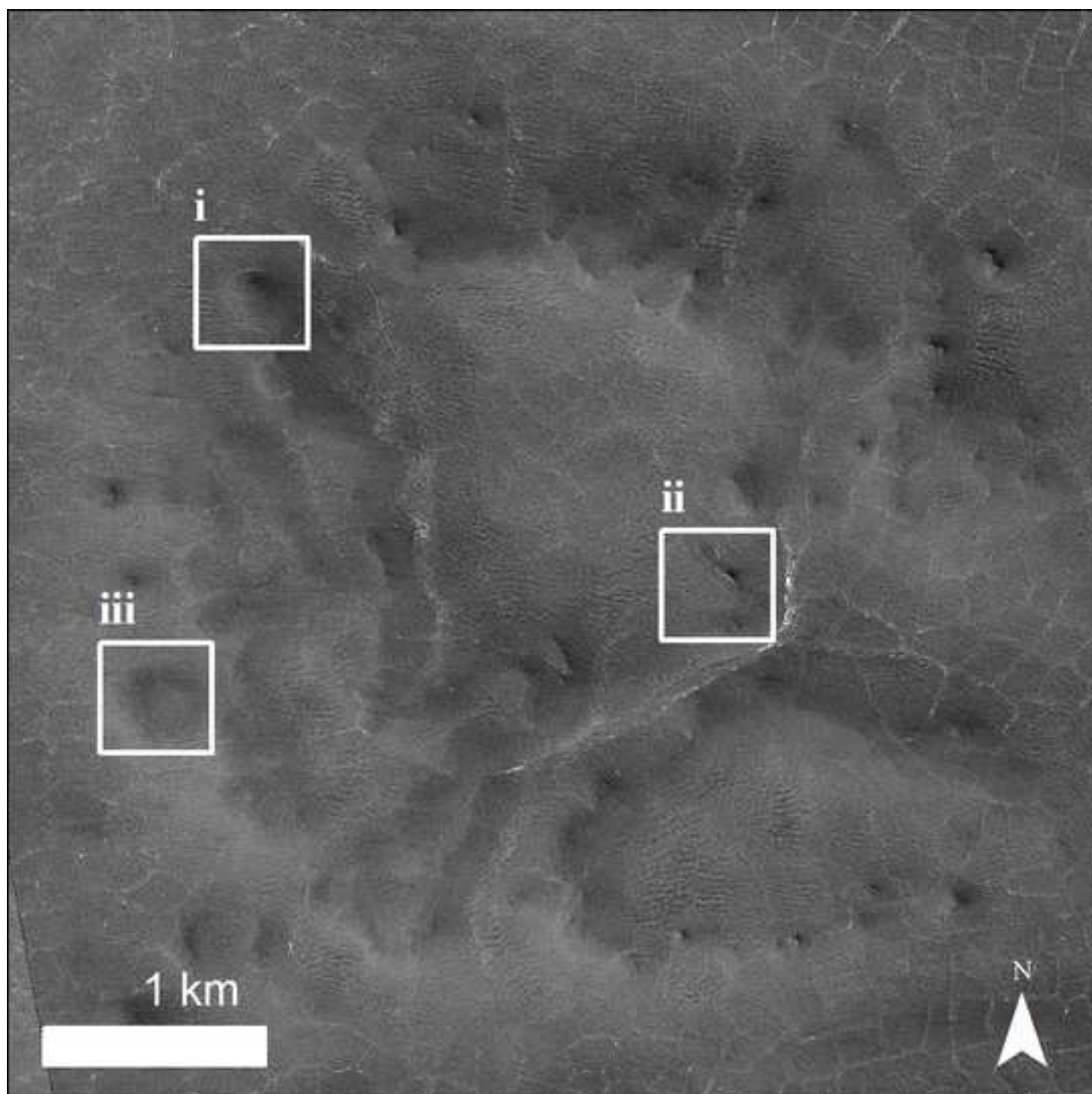


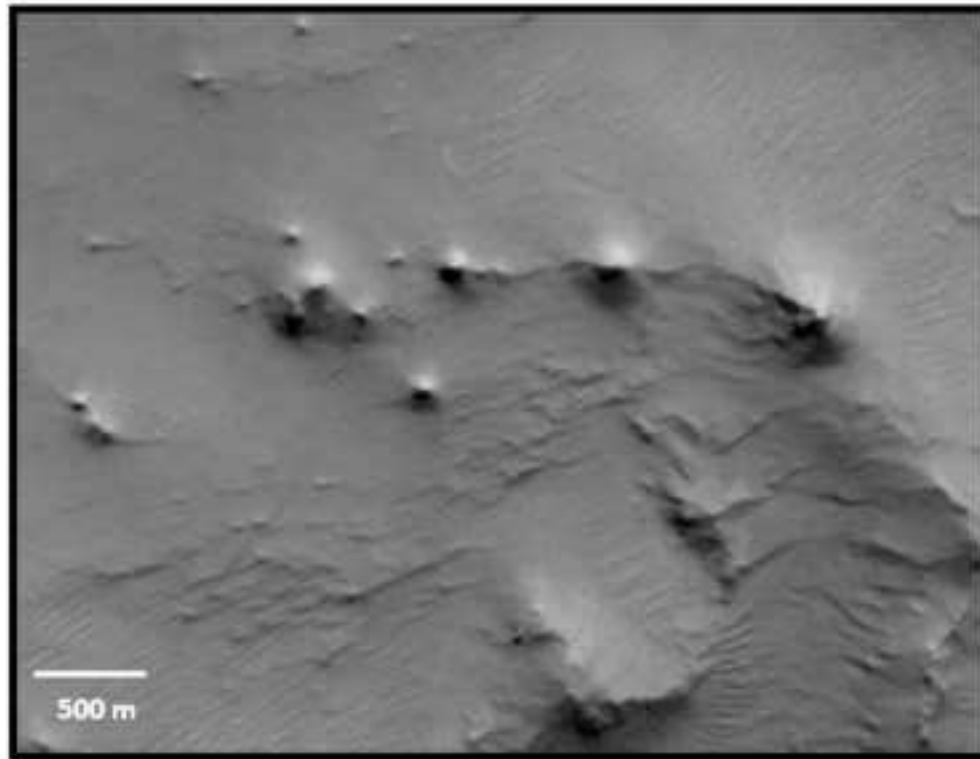
## Craters in local area to Mounds

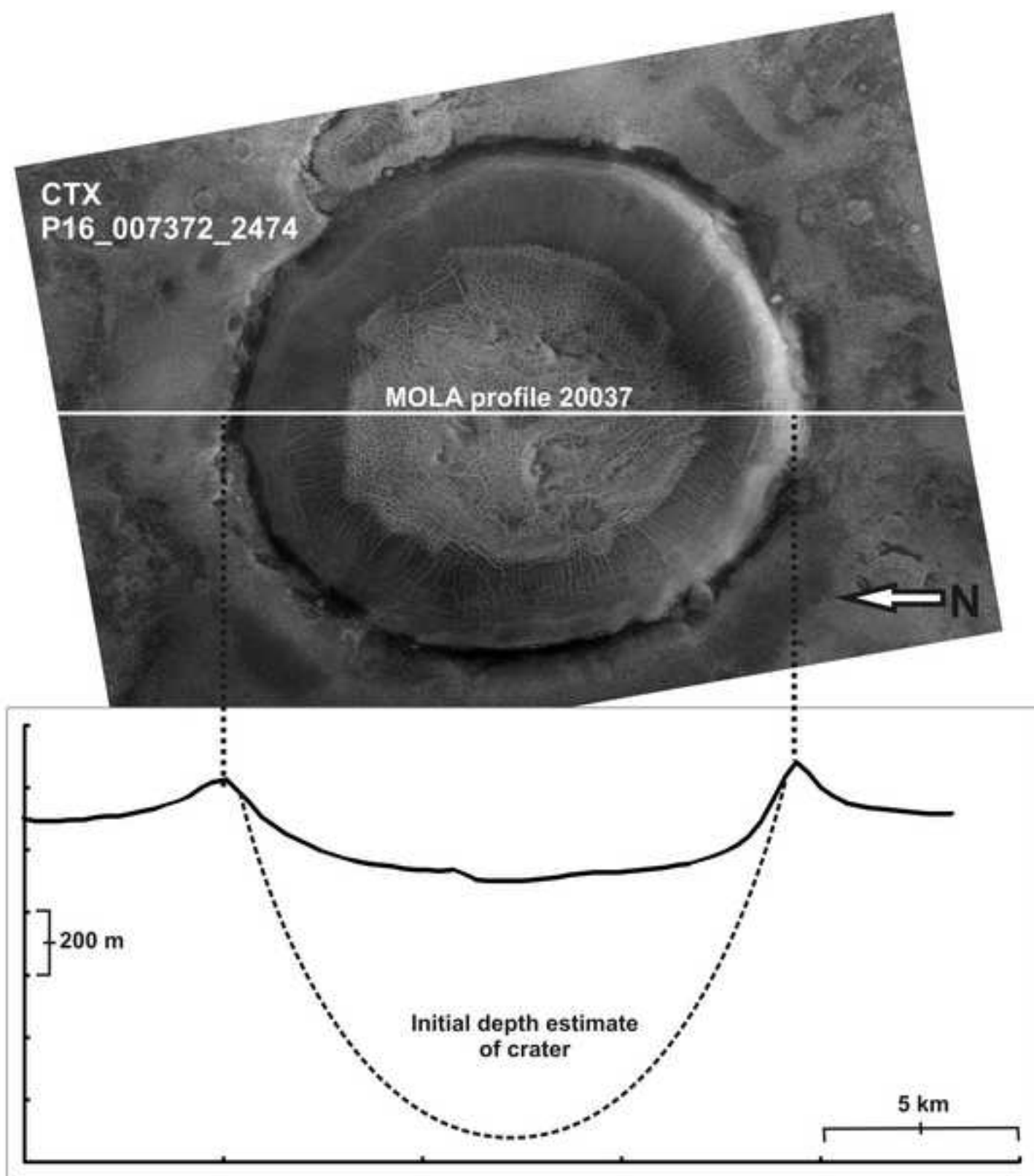




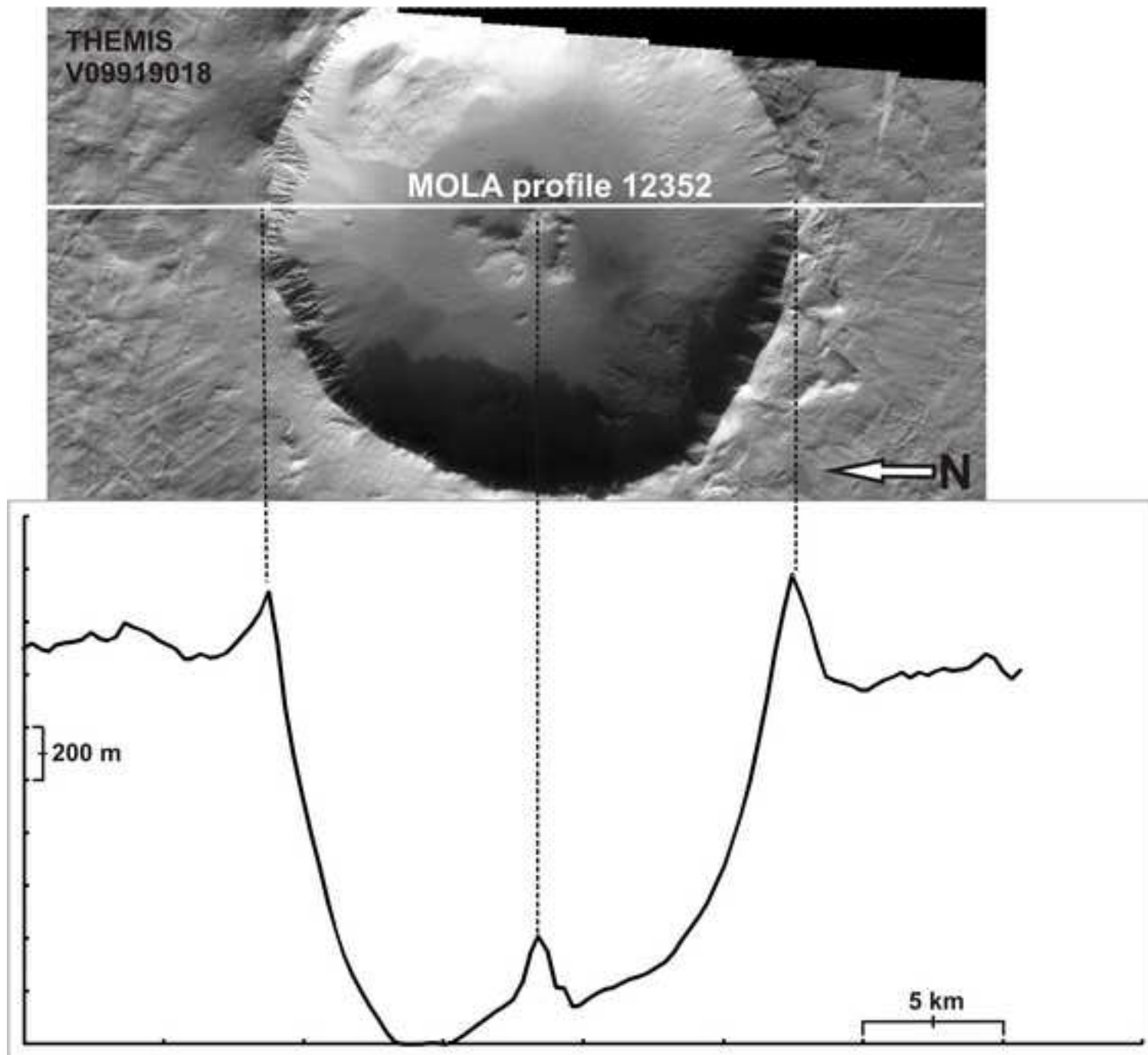




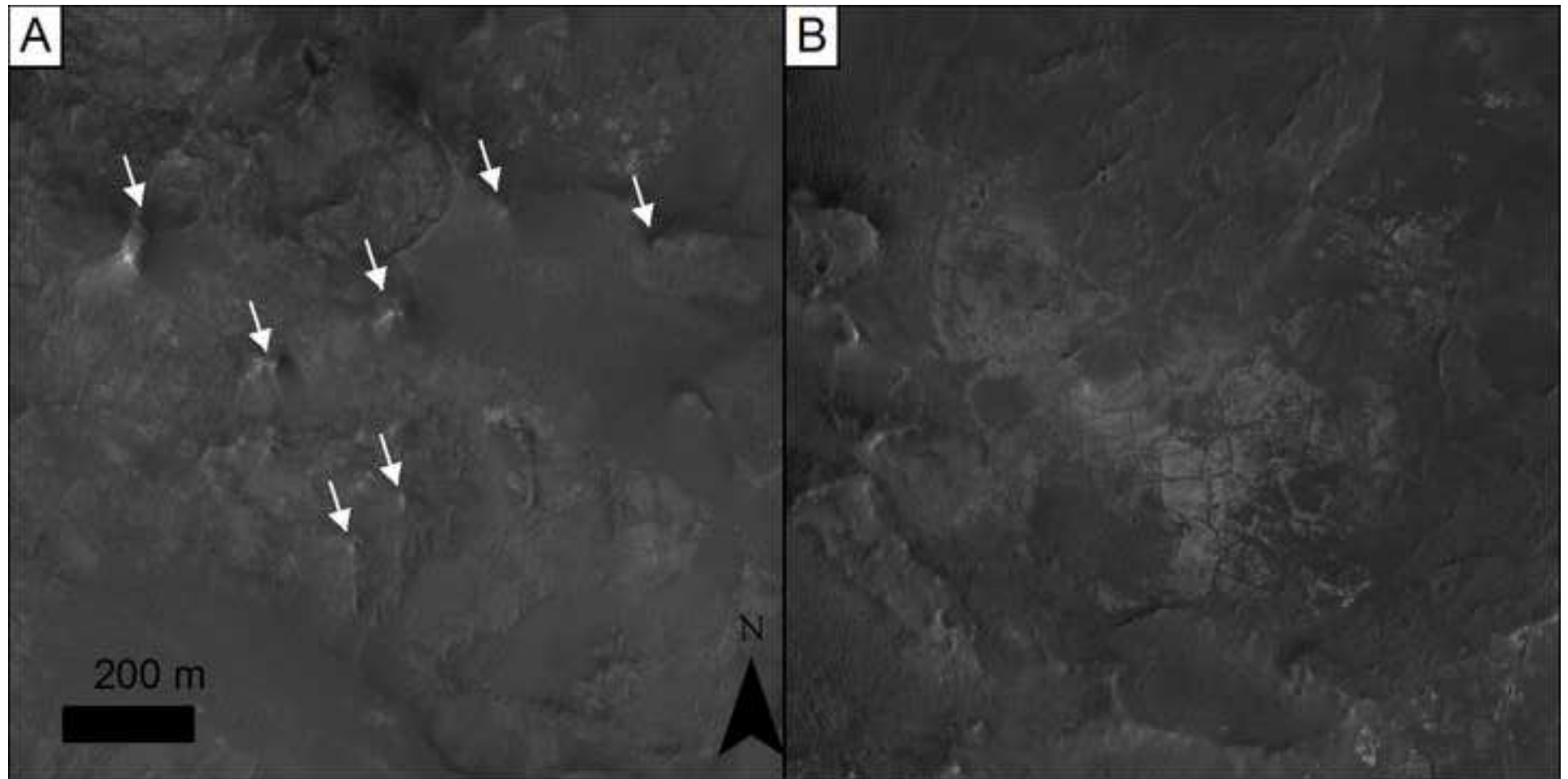














621 **Highlights**

622 >Closed-system pingos (CSPs) are perennial ice-cored mounds>They form from pooled surface  
623 H<sub>2</sub>O and by means of freeze-thaw cycling>Mound-like CSPs occur in 5 highly-filled northern  
624 near-polar impact craters on Mars>Formation hypotheses based on leading alternatives are  
625 shown to be less robust>CSPs need regional boundary-conditions to be wetter/warmer than most  
626 models predict

627

628

629

630